Volume 12; Issue 01

# PARKINSON'S DISEASE DETECTION USING DIFFERENT CNN ARCHITECTURES WITH EFFECTIVE FEATURE SELECTION APPROACH

Md. Toukir Ahmed[1*], Mohammed Sowket Ali[2] and Md. Nazrul Islam Mondal[3]

[1] IoT and Robotics Engineering, Bangabandhu Sheikh Mujibur Rahman Digital University, Bangladesh, Kaliakair, Gazipur-1750, Bangladesh
[2] Computer Science and Engineering, Bangladesh Army University of Science and Technology, Saidpur-5310, Bangladesh
[3] Computer Science and Engineering, Rajshahi University of Engineering and Technology, Rajshahi-6204, Bangladesh
*Corresponding Author: toukircse14@gmail.com

**Abstract.** The most prevalent neurological condition affecting the central nervous system is Parkinson's disease. It has been claimed that PD sufferers' handwriting deteriorates. In this sector different machine learning algorithms and techniques are applied however these have some limitations. Because of model bias generated by data inequity, these artificial intelligence architectures perform well on the vast majority however poorly on the minority class. To address this issue, we propose a model where the training process is balanced using a random under sampling strategy. The re-sampling techniques are not used on the entire dataset before cross validation, rather solely on the training phase at every cross-validation iteration. In this purpose, we use the HandPD dataset, which is divided into two sections: Spiral data and Meander data. In this study, we use CNN to extract features from handwritten dynamics photos, which collect a range of data while analyzing the subject. The HandPD dataset is divided into two portions, 25% used for testing and 75% for training. with 128*128 and 64*64 images utilized in both cases. For comparison and to discover the optimum architecture, we propose CNN Architecture 1(CA1) and CNN Architecture 2(CA2). To serve as a point of reference, we run a second experiment on the original data. Despite the fact that any machine learning methodology can be used, we pick the OPF (Optimum-Path Forest) classifier because it is quick and parameter less. We calculate the overall accuracy and average control and Parkinson Disease patient accuracies across the entire test set for each meander dataset and spiral dataset separately. CA1 performs better in terms of total accuracy averaged for the test set when using the meander dataset, with accuracy of 87.24% and 85.10% for 128*128 and 64*64 images, respectively. For average Performance of Patients with Parkinson disease throughout test set using the meander dataset, we find that OPF performs better, with 93.66% and 91.66% accuracy for 128*128 and 64*64 images, respectively. Average overall accuracy across all test sets in the case of the Spiral dataset, we discover that OPF performs better, with an accuracy of 76.82% for 128*128 images, and CA1 performs better, with an accuracy of 81.19% for 64*64 images. Accuracies over the test set for average PD patients in the case of the Spiral dataset, we discover that CA2 performs better, with an accuracy of 90.89 percent for 128*128 images, while CA1 performs better, with an accuracy of 87.68 percent for 64*64 images. Experiments show that different CNN architectures are better in different scenarios. However, in the great majority of situations, CA1 performs better.

**Keywords:** Machine Learning, Parkinson's disease, Imbalanced data, CNN, Feature and HandPD dataset.

## 1. Introduction and Motivation

One of the most common neurological disorders, Parkinson's disease, affects more than 1% of people over the age of sixty [1]. This neurodegenerative condition is marked by motor problems such tremor, bradykinesia, stiffness, and postural instability and is caused by the loss of dopaminergic function [2]. Motor

Submitted: March 31, 2023
Accepted: June 21, 2023
https://doi.org/10.59185/6.12.05.53-64

planning, coding, and synchronization are all impacted, as well as movement initiation and execution.[3]. The symptoms of Parkinson's disease are the fourteenth largest cause of mortality in the US, according to the Centers for Disease Control and Prevention. With reality, there are currently over 10 million Parkinson's patients worldwide. It should be underlined that early Parkinson's disease discovery, as indicated in [4], enables prompt treatment and considerably reduces symptoms. Therefore, diagnosing PD at an early stage is essential to halting its development and may give patients access to disease-modifying drugs once they become available. The need of early diagnosis of PD should be highlighted because doing so can drastically reduce one's quality of life, especially for the elderly. Diagnostic criteria based on motor symptom evaluation are now used to make this determination. In order to help in PD diagnosis, Pereira et al. [5–9] recently created machine learning and computer vision architectures. Pereira et al. gathered information from there were 55 people in all, with 37 PD sufferers and 18 healthy people topics [5]. Only spiral drawings were included in the dataset. They used supervised models like SVM, Optimal Path Forest (OPF) and Naive Bayes to distinguish between PD patients' handwritten drawings and those of healthy people. With the NB model, they got the highest accuracy of 78.9%. They created a new dataset from 18 healthy volunteers and 74 Parkinson's disease patients for future studies [10]. The collection is called HandPD, and it contains 736 samples, making it the largest publicly available handwritten dataset to date. The same approaches SVM, OPF, and NB are used to extract characteristics from handwriting drawing made using machine learning methods, employed for classification on the HandPD dataset. For the HandPD dataset, they attained a classification accuracy of 67%. In studies using the HandPD dataset, there are two major issues. This reflects model bias and a low percentage of PD detection accuracy. Other studies, such as Pan et al[11], evaluated RBF and SVM for the start of shaking in Parkinson's disease sufferers. Later, Hariharan et al. [13] created an innovative feature weighting procedure based on Model-based clustering to enhance the discriminating power of dysphonia-based characteristics, achieving 100% classification performance. In order to aid in the diagnosis of Parkinson disease, Peker et al. [12] employed complicated neural network models and sound-based characteristics. To deal with PD identification, the majority of studies use audio-based datasets. Pereira et. al.[14] proposed handwriting gestures to improve PD diagnosis. Same investigators posted a database online that contained 100 of images of handwritten doodles created by healthy and unwell individuals. Because Parkinson's disease impairs writing ability, such tests are utilized in medical centers, but only a few studies have investigated them for the purposes of automated identification. A few years in the past, Peuker et al. [15] successfully conducted PD detection using the signals obtained from the ballpoint. Although, the writers did use a sequentially driven feature selection approach to extract about four hundred manually created characteristics from the signal, which might be too costly.

## 2. Dataset Description and Problem Identification

Parkinson's disease sufferers' writing is frequently distorted and shorter than that of healthy people due to tremors, diminished motion vibrations, latency, and hardness [16]. Nowadays, it is challenging to establish a single diagnostic that will able to recognize an abnormal in the initial phases.

Parkinson's disease can occasionally be confused with a number of different brain illnesses. This study made use of the HandPD dataset, which is freely accessible online [17]. The information was received from ninety-two persons at Sao Paulo State University's Botucatu Faculty of Medicine. The data came from two groups of people: 74 PD sufferers and 18 healthy people. The first group consists of fifty-nine male and fifteen female individuals, whereas the next group consists of six male and twelve female subjects. As a result, healthy people make up 19.56 percent of the total dataset, while PD patients make up 80.44 percent. A total of 2 left-handed and 16 right-handed patients make up the control group. Patients with Parkinson's disease, nonetheless, are composed of sixty-nine right-handed people and five left-handed people. Each subject was asked to complete six distinct activities during the data collecting process, as indicated in Fig. 1. The picture is a form drawn by a 56-year-old Parkinson's disease patient. The HandPD dataset only includes the meander and spiral designs as two of the six possible locations. Each theme produced four spirals and four meanders. Thus, the dataset has 92 * 8 = 736 drawings. 368 of the designs—or half—are spirals, and the remaining 144 are meanders. To determine a person's skills when completing a form like the one in Picture 1, Pereira et al. [18] created a dataset of handwriting exam images. The form's objective is to request completion of a number of specific activities that are regarded to be challenging for those with Parkinson's disease, Building "spirals" and "meanders" are two examples; row 'c' and row 'd' in Fig. 1 respectively.

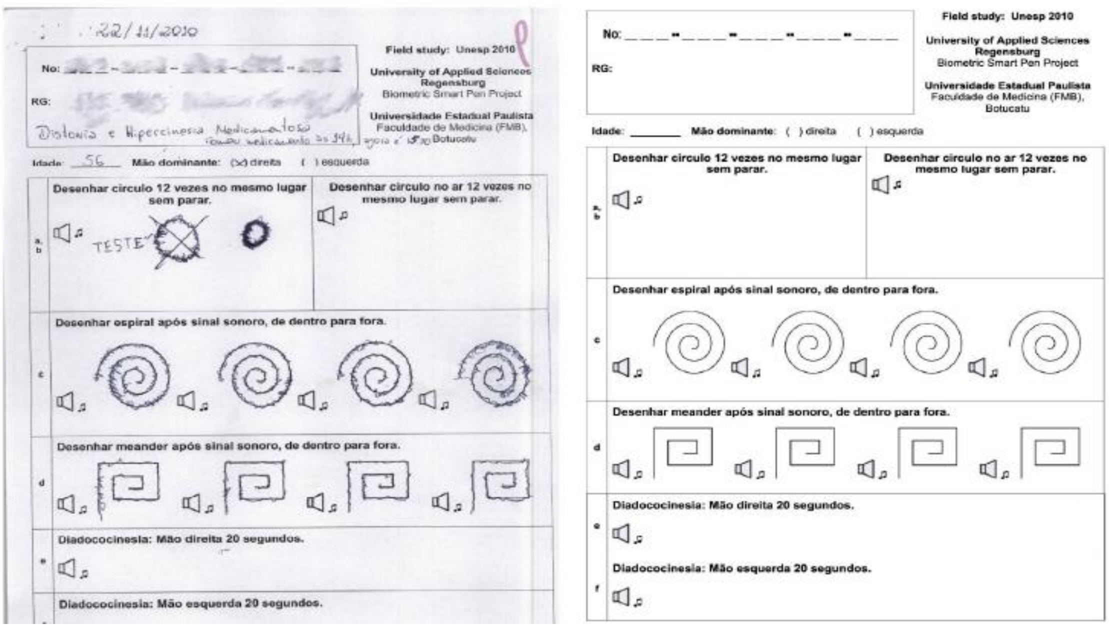


**Fig. 1.** (a) A form filled out by a fifty-six year-old Parkinson's disease sufferers, (b) an example of a blank form

In this part, we will look at two major issues with the dataset. The uneven nature of the data is the first issue, and it has an effect on the developed mathematical models for machine learning. Machine learning architectures that are trained on skewed data have skewed productivity because they neglect the minority group and elevate the dominant class [19]. Due to the rarity of minority class incidents during the training process, projections for minorities are also uncommon, undiscovered, or overlooked [20]. Convolutional neural networks have not before been used to learn characteristics from artwork generated by handwritten dynamics, which gather a variety of data while evaluating a person. We also want to point out that the purpose of this research is not to compare and uncover the best CNN architecture. Another essential point to note is that these studies do not calculate the average overall accuracy as well as the average control and PD patient accuracies for each meander and spiral data set individually over the test set.

## 3. Methodology

We recommend utilizing CNNs to simulate the identification of PD and normal individuals as an image identification task. In a nutshell, the digital pen's impulses are translated into visuals. Every test consists of r rows (duration of the test in ms) and six columns (the previously mentioned six signals channel). In order to achieve our goals, every test must be expanded to a square matrices. After rescaling, every test matrix is balanced and represented as a gray-scale image. We display various sketches together with their transformed equivalents as time series images. Drawings of meanders and spirals, as well as those of people in good health and those with Parkinson's, all show variances. A CNN-based method was used to classify the meanders and spirals produced by the study's control subjects and PD patients. As a benchmark, we also conduct a unique analysis on the raw data. The OPF classification algorithm is chosen despite the fact that any supervised machine learning technique can be used because of its speed and lack of parameters [21,22]. In this study, Caffe offers a clean and flexible framework for cutting-edge deep learning algorithms as well as a set of reference models. Additionally, it permits experimentation and easy platform swapping for deployment from prototyping devices to cloud environments. Meanders and spirals are the two datasets used for the experiments. There are 308 photos in both datasets, with there have been two hundred and twenty four Parkinson patients and eighty four normal group samples in this study. We also put the convolutional neural network through their paces at 64*64 and 128*128 pixel image resolutions. During one experiment, we also investigate the effects of the training set's size by using 75% of the dataset for learning and 25% for evaluation. In terms of original code, the well-known Caffe library is used [23], On the Graphics Processor Units platform, it is designed for general-purpose computing. Consequently, more efficient implementations are possible. Each experiment is assessed using a separate Caffe-provided CNN architecture with ten thousand training iterations and sixteen-bit mini-batches are used in this experiment. We cross-validate using twenty runnings to offer a data study using the Wilcoxon signed-rank check with such a value of 0:05 [24]. To give a more in-depth experimental investigation, CA1 and CA2 CNN architectures are proposed.After getting the final result from experimental setup then we compare the architectures and try to find out the best architecture.Finally we turn a conclusion and find out the future work.

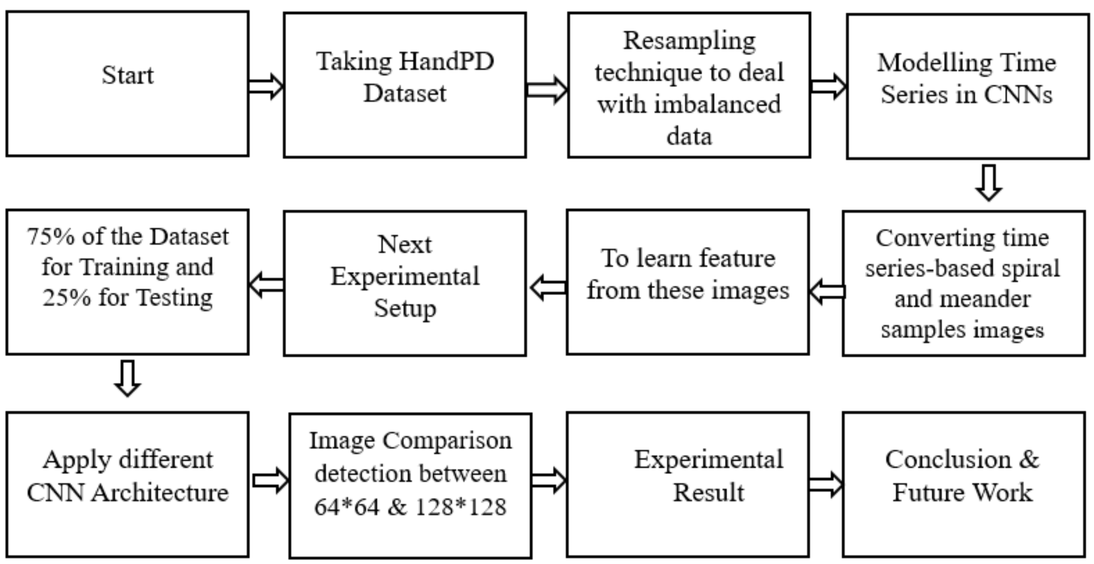


**Fig. 2.** Proposed Methodology

The following are some of the retrieved features from HandPD data set [25, 26]:

C1: The difference between the Hand written trace and Exam template radius's Root Mean Square , which is calculated using the following formula:

$$\text{RMS}=\sqrt{\frac{1}{n}\sum_{i=1}^{n}(r_{HT}^{i}-r_{ET}^{i})} \tag{1}$$

Whrere n= number of sampled points, $r_{HT}^{i}$ = the Hand written trace radius of i-th point and $r_{ET}^{i}$ = the Exam template radius of i-th point.

C2: The biggest difference between Hand written trace and Exam template radius is the second characteristic, which is calculated using the formula:

$$dis_{\max = \arg max_i\{|r_{HT}^i - r_{ET}^i|\}} \tag{2}$$

C3: This feature is the lowest difference between Hand written trace and Exam template radius, which is provided by dmin in the following equation:

$$dis_{\min = \arg min_i\{|r_{HT}^i - r_{ET}^i|\}} \tag{3}$$

C4: The next feature is the standard deviation of the difference between Hand written trace and Exam template radius.

C5: Mean Relative Tremor is the fifth characteristic (MRT). This aspect was suggested by Pereira et al. to assess a person's HT's level of tremor [30]. It is the standard deviation of the distance between a sample point's radius and its d left-nearest neighbors' radius. The following formula is used to calculate this feature:

$$\text{MRT}= \frac{1}{n-d} \sum_{i=d}^{n} |\, r_{ET}^{i} - r_{ET}^{i-d+1} | \tag{4}$$

Where d stands for the separation of the sample sites from which the radius variation was calculated. The relative tremor $|r_{ET}^{i} - r_{ET}^{i-d+1}|$ is used to calculate the next three features.

C6: The maximum ET is indicated by the sixth characteristic.

C7: The minimum ET is indicated by the seventh characteristic.

C8: The eighth feature is the typical derivation of Exam template values.

C9: The last feature is the frequency with which the difference between the Exam pattern radius and the Handwritten trace changes from positive to negative, or vice versa.

After analyzing the provided dataset and making it acceptable for machine learning techniques, we used two resampling strategies that depend on changing the class distribution. We currently perform the following actions with the unbalanced HandPD dataset:

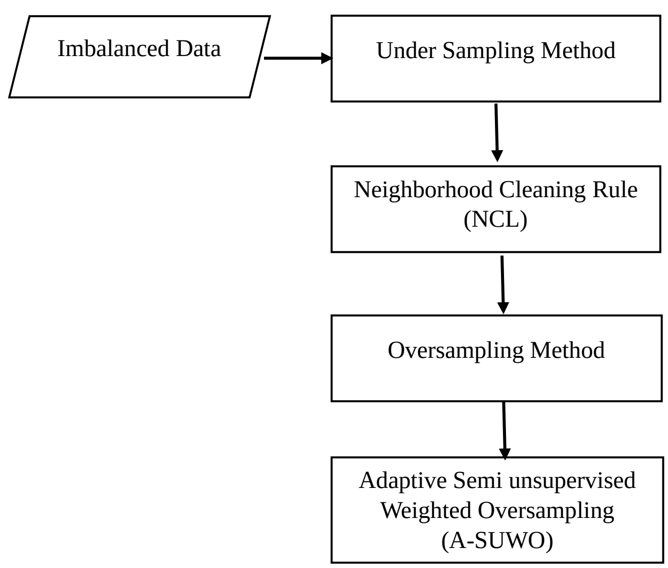


**Fig. 3.** Flowchart of Balancing the HandPD data set

First, we use the HandPD dataset that is available online, followed by an undersampling technique called Neighborhood Cleaning Rule (NCL), and an oversampling technique called Adaptive Semiunsupervised Weighted Oversampling (A-SUWO). In order to handle this unbalanced dataset, we employ a hybrid oversampling/undersampling technique.

Throughout this study, we use a Convolutional neural approach to classify meanders and spirals produced by the healthy controls and Parkinson patients. We conduct a second test using the original data as a baseline. Any supervised machine learning algorithm can be utilized, though, because it is a rapid and parameter-free technique, we choose the OPF classifier [27], [28]. Two datasets were created from the research: (i) meanders and (ii) spirals. 84 samples from the normal control and 224 samples from PD sufferers total 308 images in both groups. We also tested the reliability of CNNs at two distinct quality of images: 64 *64 and 128* 128 pixels. The HandPD dataset was divided into two portions: 25% for testing and 75% for training. The implementations are more effective because the source code was written using the well-known Caffe library [29]. 10,000 learning cycles using 16-piece mini-batches and a distinct Convolutional Architecture for Fast Feature Embedding provided CNN architecture were utilized to assess each experiment. With 20 running, we performed a cross-validation. In order to give a more experimental investigation, various CNN architectures were used:

*CNN Architecture 1(CA1):*
This design is made up of five pooling layers, five convolution layers, five pooling layers, and two normalizing layers. It has five inner product layers, five ReLU layers, one soft max loss layer, two dropout levels and one accuracy layer for testing among the convolutional layers.

*CNN Architecture 2(CA2):*
Three pooling layers and three convolution layers are used in a simpler version. It has three ReLU layers, one soft max loss layer, two inner product layers, and for the testing purposes one accuracy layer is used.

## 1. Experimental Findings

In this chapter,we dicuss the experimental details result with proper tabuler formet. We calculate the overall accuracy with the help of following formula:

$$\text{Accuracy}=\left(\mathbf{1}-\frac{\boldsymbol{errors}}{\boldsymbol{dataset\ size}}\right)*\mathbf{100} \tag{5}$$

In this section, **t**wo different CNN architectures were compared**,** and a baseline method using the OPF learning algorithm with both spiral and meander collections**.** For all cases, we consider the 75% for training data and 25% for testing data**.**

**Table 1.** Considering the Meander Dataset, average overall accuracy over the test set

| | 128 *128 | 64 *64 |
|---|---|---|
| CA1 | **87.24%** | **85.10%** |
| CA2 | 63.22% | 68.88% |
| OPF | 81.92% | 84.52% |

In table 1 we calculate, considering the Meander Dataset, overall average of the test set's accuracy. Here we take the 128*128 and 64*64 sizes images. We see that for 128*128 images the CA1, CA2 and OPF accuracy are 87.24%, 63.22%, 81.92% respectively. We also observe that for 64*64 images the CA1, CA2 and OPF accuracy are 85.10%, 68.88%, 84.52% respectively. Here the best performer is CA1 for the both cases.

**Table 2.** Average PD Patient Accuracy across the Test Set Using Meander Dataset

| | 128 *128 | 64 *64 |
|---|---|---|
| CA1 | 91.55% | 89.65% |
| CA2 | 85.20% | 82.24% |
| OPF | **93.66%** | **91.66%** |

In table 2 we calculate average PD Patient Accuracy Across The Test Set Using Meander Dataset. Here we take the 128*128 and 64*64 sizes images. We see that for 128*128 images the CA1,CA2 and OPF accuracy are 91.55%, 85.20%, 93.66% respectively. We also observe that for 64*64 images the CA1,CA2 and OPF accuracy are 89.65%, 82.24%, 91.66% respectively. Here the best performer is OPF for the both cases. But if we consider the CA1 and CA2, here in these two, CA1 is best.

**Table 3.** Mean Total Accuracy Including Spiral Dataset Well over Test Set

| | 128 *128 | 64 *64 |
|---|---|---|
| CA1 | 76.53% | **81.19%** |
| CA2 | 71.78% | 77.21% |
| OPF | **76.82%** | 78.32% |

In table 3 we calculate Mean Total Accuracy Including Spiral Dataset Well Over Test Set. Here we take the 128*128 and 64*64 sizes images. We see that for 128*128 images the CA1,CA2 and OPF accuracy are 76.53%, 71.78%, 76.82% respectively. We also observe that for 64*64 images the CA1,CA2 and OPF accuracy are 81.19%, 77.21%, 78.32% respectively. Here the best performer is CA1 for the 64*64 image and OPF is best for 128*128 images. But if we consider the CA1 and CA2, here in these two, CA1 is best for 128*128 images.

**Table 4.** Mean PD Individuals Accuracy across the Test Set Using Spiral Data

| | 128 *128 | 64 *64 |
|---|---|---|
| CA1 | 84.80% | **87.68%** |
| CA2 | **90.89%** | 84.33% |
| OPF | 83.24% | 86.45% |

In table 4 we calculate Mean PD Individuals Accuracy across the test set using spiral data. Here we take the 128*128 and 64*64 sizes images. We see that for 128*128 images the CA1, CA2 and OPF accuracy are 84.80%, 90.89%, 83.24% respectively. We also observe that for 64*64 images the CA1, CA2 and OPF accuracy are 87.68%, 84.33%, 86.45% respectively. Here the best performer is CA1 for the 64*64 image and CA2 is best for 128*128 images. Tables 1, 2, 3, and 4 are depicted in Fig. 4, 5, 6, and 7, respectively. Here we get the clear view and find the clear findings of this research.

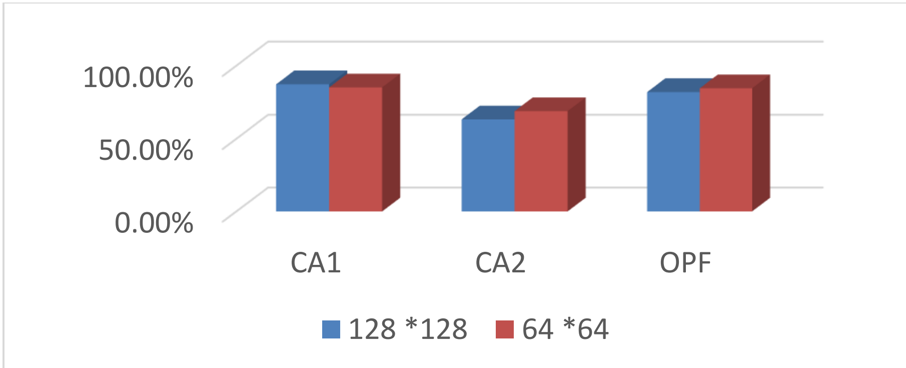


**Fig. 4.** Considering the Meander Dataset, overall average of the test set's accuracy.

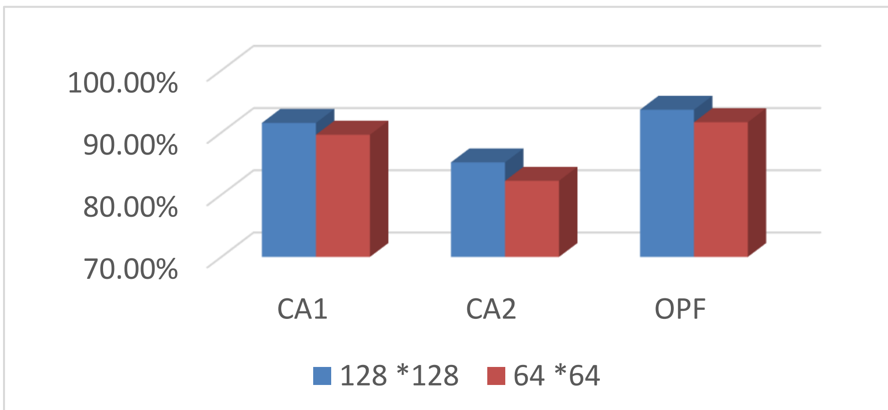


**Fig. 5.** Average PD Patient Accuracy across the Test Set Using Meander Dataset

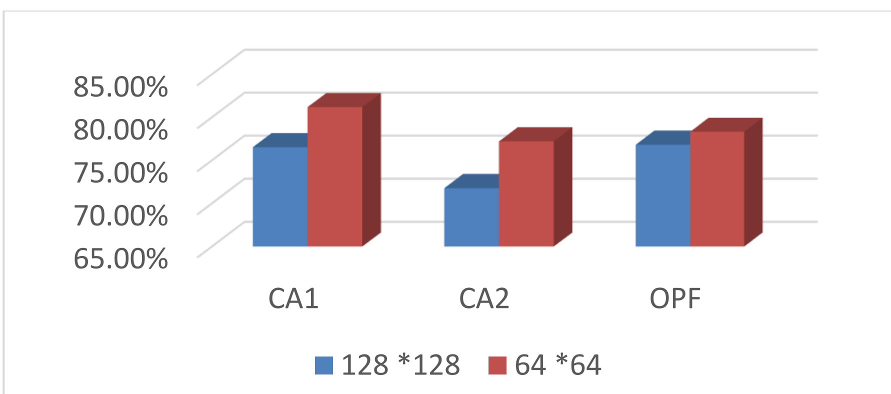


**Fig. 6.** Mean Total Accuracy Including Spiral Dataset Well over Test Set

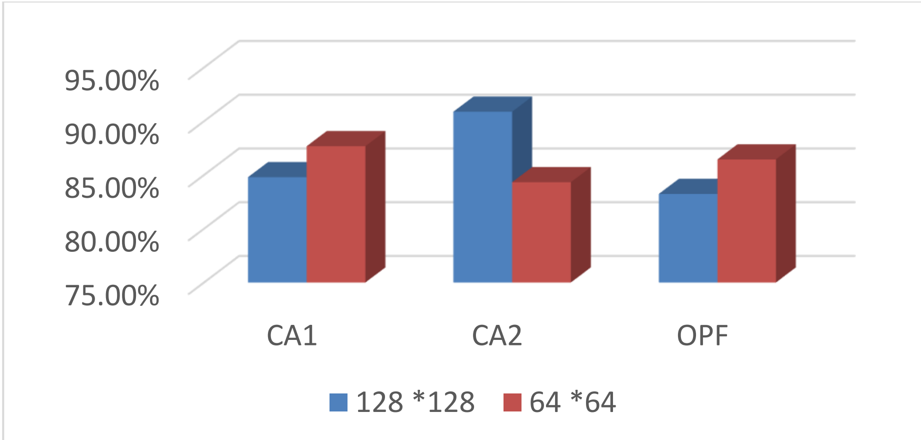


**Fig. 7.** Mean PD Individuals Accuracy Across the Test Set Using Spiral Data.

Ten study summaries for Parkinson's disease were supplied in the introduction and motivation section; presently, it is clear that CA1 outperforms these algorithms, and in some cases, CA2 as well.

## 2. Conclusion

An illness that affects the central nervous system is called Parkinson's disease, is brought on by the death of brain cells. Trembling, tremors, stiffness, difficulty walking, and loss of hand control are the early symptoms of the condition. Since Parkinson's illness is incurable, early detection is important. In this sector different machine learning algorithms and different techniques are applied however these have some limitations. Because of model bias generated by data that is unbalanced, these Models for machine learning perform well on the the vast majority however poorly on the minority class. To address this issue of biasness, we propose a model that the training process be balanced using a random under sampling strategy. The resampling techniques are not used on the entire dataset before cross validation, but rather solely on the training examples at every cross-validation iteration. We use the HandPD data set, which is divided into two sections: Spiral data and Meander data. CNNs are used in this study to extract properties from images produced by handwritten movements, which collect data as the topic is being studied. The HandPD dataset is divided into two portions, with 25% used for testing and 75% for training. With 128*128 and 64*64 images (chosen at random, not for any particular reason) utilized in both cases. Each experiment is run with 10,000 training iterations and 16-bit mini-batches using different CNN architectures given by Caffe. With 20 running's, we perform a cross-validation. For comparison and to discover the optimum architecture, we propose CNN Architecture 1(CA1) and CNN Architecture 2(CA2). To serve as a point of reference, we also conduct a different experiment on the unprocessed data. Any machine learning methodology can be applied, though. We pick the OPF (Optimum-Path Forest) classifier because it is a quick and parameter less method. We calculate the average overall accuracy and the average sufferer with Parkinson's disease and the average normal accuracies over the test set for each meander data set and spiral data set separately. CA1 performs better in terms of total accuracy averaged over the full test set when using the meander dataset, with accuracy of 87.24 percent and 85.10 percent for 128*128 and 64*64 images, respectively. Accuracy rate over the test set for typical Patients with PD using the meander data, we find that OPF performs better, with 93.66 percent and 91.66 percent accuracy for 128*128 and 64*64 images, respectively. Average overall accuracy across all test sets in the case of the Spiral dataset, we discover that OPF performs better, with an accuracy of 76.82 percent for 128*128 images, and CA1 performs better, with an accuracy of 81.19 percent for 64*64 images.

Accuracies over the test set for average PD patients in the case of the Spiral dataset, we discover that CA2 performs better, with an accuracy of 90.89 percent for 128*128 images, while CA1 performs better, with an accuracy of 87.68 percent for 64*64 images. Experiments show that different CNN architectures are better in different scenarios. Nonetheless, CA1 consistently outperforms other methods.

## References


1. Tysnes, O.B.; Storstein, A. Epidemiology of Parkinson's disease. J. Neural Transm. 2017, 124, 901–905.
2. R. Prashanth and S. D. Roy, "Early detection of parkinson's disease through patient questionnaire and predictive modelling," International journal of medical informatics, vol. 119, pp. 75–87, 2018.
3. Armstrong MJ, Okun MS. Diagnosis and treatment of Parkinson disease. JAMA 2020;323:548–60.
4. N. Singh, V. Pillay, and Y. E. Choonara, "Advances in the treatment of parkinson's disease," Progress in neurobiology, vol. 81, no. 1, pp. 29–44,2007.
5. C. R. Pereira, D. R. Pereira, F. A. Silva, J. P. Masieiro, S. A. Weber, C. Hook, and J. P. Papa, ``A new computer vision-based approach to aid the diagnosis of Parkinson's disease," Comput. Methods Programs Biomed., vol. 136, pp. 79_88, Nov. 2016.
6. C. R. Pereira, L. A. Passos, R. R. Lopes, S. A. Weber, C. Hook, and J. P. Papa, ``Parkinson's disease identi_cation using restricted Boltzmann machines," in Proc. Int. Conf. Comput. Anal. Images Patterns. Springer, 2017, pp. 70-80.
7. C. R. Pereira, S. A. T. Weber, C. Hook, G. H. Rosa, and J. P. Papa, ``Deep learning-aided parkinson's disease diagnosis from handwritten dynamics," in Proc. 29th SIBGRAPI Conf. Graph., Patterns Images (SIBGRAPI), 2016, pp. 340-346.
8. C. R. Pereira, D. R. Pereira, S. A.Weber, C. Hook,V. H. C. de Albuquerque, and J. P. Papa, ``A survey on computer-assisted Parkinson's disease diagnosis," Artif. Intell. Med., vol. 95, pp. 48_63, Apr. 2019.
9. S. Pan, S. Iplikci, K. Warwick, and T. Z. Aziz, "Parkinson's disease tremor classification, a comparison between support vector machines and neural networks," Expert Systems with Applications, vol. 19, pp. 10 764–10 771, 2012.
10. Marras C, Lang A, van de Warrenburg BP, et al. Nomenclature of genetic movement disorders: recommendations of the International Parkinson and movement disorder Society Task force. Mov Disord 2016;31:436–57.
11. M. Peker, B. Sen, and D. Delen, "Computer-aided diagnosis of parkinson's disease using complex-valued neural networks and mRMR feature selection algorithm," Journal of Healthcare Engineering, vol. 6, no. 3, pp. 281–302, 2015.
12. M. Hariharan, K. Polat, and R. Sindhu, "A new hybrid intelligent system for accurate detection of parkinson's disease," Computer Methods and Programs in Biomedicin, vol. 11, no. 3, pp. 904–913, 2014.
13. S. Rosenblum, M. Samuel, S. Zlotnik, I. Erikh, and I. Schlesinger, ``Handwriting as an objective tool for Parkinson's disease diagnosis," J. Neurol., vol. 260, no. 9, pp. 2357_2361, 2013.
14. C. R. Pereira, D. R. Pereira, F. A. da Silva, C. Hook, S. A. T. Weber, L. A. M. Pereira, and J. P. Papa, "A step towards the automated diagnosis of parkinson's disease: Analyzing handwriting movements," in IEEE 28th International Symposium on Computer-Based Medical Systems, 2015, pp. 171–176.
15. D. Peuker, G. Scharfenberg, and C. Hook, "Feature selection for the detection of fine motor movement disorders in parkinson's patients," in Advanced Research Conference, ser. ARC '11. Shaker Verlag, 2011.
16. Mantri S, Morley JF, Siderowf AD. The importance of preclinical diagnostics in Parkinson disease. Parkinsonism Relat Disord 2019;64:20–8.
17. C. R. Pereira, D. R. Pereira, F. A. Silva, J. P. Masieiro, S. A. Weber, C. Hook, and J. P. Papa. (2016). Handpd Dataset. Accessed: Jun. 15, 2021.
18. C. R. Pereira, D. R. Pereira, F. A. da Silva, C. Hook, S. A. T. Weber, L. A. M. Pereira, and J. P. Papa, "A step towards the automated diagnosis of parkinson's disease: Analyzing handwriting movements," in IEEE 28th International Symposium on Computer-Based Medical Systems, 2015, pp. 171–176.
19. Y. Wang, A.-N. Wang, Q. Ai, and H.-J. Sun, ``An adaptive kernelbased weighted extreme learning machine approach for effective detection of Parkinson's disease," Biomed. Signal Process. Control, vol. 38, pp. 400–410, Sep. 2017.
20. Y. Sun, A. K. Wong, and M. S. Kamel, ``Classi_cation of imbalanced data: A review," Int. J. Pattern Recognit. Artif. Intell., vol. 23, no. 4, pp. 687_719, 2009. doi: 10.1142/S0218001409007326.

21. J. P. Papa, A. X. Falc˜ao, and C. T. N. Suzuki, “Supervised pattern classification based on optimum-path forest,” International Journal of Imaging Systems and Technology, vol. 19, no. 2, pp. 120–131, 2009.
22. J. P. Papa, A. X. Falc˜ao, V. H. C. Albuquerque, and J. M. R. S. Tavares, “Efficient supervised optimum-path forest classification for large datasets,” Pattern Recognition, vol. 45, no. 1, pp. 512–520, 2012.
23. Y. Jia, E. Shelhamer, J. Donahue, S. Karayev, J. Long, R. Girshick, S. Guadarrama, and T. D. T., “Caffe: Convolutional architecture for fast feature embedding,” arXiv preprint arXiv:1408.5093, 2014.
24. F. Wilcoxon, “Individual comparisons by ranking methods,” Biometrics Bulletin, vol. 1, no. 6, pp. 80–83, 1945.
25. C. R. Pereira, D. R. Pereira, F. A. da Silva, C. Hook, S. A. Weber, L. A. Pereira, and J. P. Papa, ``A step towards the automated diagnosis of Parkinson's disease: Analyzing handwriting movements,'' in Proc. IEEE 28th Int. Symp. Comput.-Based Med. Syst., Jun. 2015, pp. 171–176.
26. C. R. Pereira, D. R. Pereira, F. A. Silva, J. P. Masieiro, S. A. Weber, C. Hook, and J. P. Papa, ``A new computer vision-based approach to aid the diagnosis of Parkinson's disease,'' Comput. Methods Programs Biomed., vol. 136, pp. 79–88, Nov. 2016.
27. J. P. Papa, A. X. Falc˜ao, and C. T. N. Suzuki, “Supervised pattern classification based on optimum-path forest,” International Journal of Imaging Systems and Technology, vol. 19, no. 2, pp. 120–131, 2009.
28. J. P. Papa, A. X. Falc˜ao, V. H. C. Albuquerque, and J. M. R. S. Tavares, “Efficient supervised optimum-path forest classification for large datasets,” Pattern Recognition, vol. 45, no. 1, pp. 512–520, 2012.
29. Y. Jia, E. Shelhamer, J. Donahue, S. Karayev, J. Long, R. Girshick, S. Guadarrama, and T. D. T., “Caffe: Convolutional architecture for fast feature embedding,” arXiv preprint arXiv:1408.5093, 2014.